CHAPTER IV

Determination of Rotational Viscosity in the Smectic C* and Smectic A Phases

4.1 Introduction

Ferroelectric liquid crystals[1] (FLC) have attracted attention owing to their fast electrooptic switching properties, two or three orders of magnitude faster than those of nematic liquid crystals.[2] Thus for certain applications which require fast electrooptic switching characteristics FLCs arc extremely useful. One of tlie important material properties which controls tlie speed of this switching is the rotational viscosity (γ_ϕ) associated with tlie motion around tlie smectic C cone."

Several methods[4-10] have been developed to determine γ_ϕ. However a detailed comparison of the values obtained by the different techniques does not seem to have been made. Moreover, there are hardly any systematic studies[11,12] as a function of the alkyl chain length of the molecule. Keeping this in view we have measured the rotational viscosity by different techniques. Tlie results show that under proper experimental conditions, all the methods give the *same* value of rotational viscosity within the experimental errors. Measurements made on different members of a

homologous series show a systematic variation with changing alkyl chain length. We have also measured the soft mode rotational viscosity[9,13] γ_s by dielectric methods.

The scheme of presentation in this chapter is as follows. First, a brief description of the concept of rotational viscosity of nematic liquid crystals is given, followed by the origin of different rotational viscosities of the ferroelectric smectic C* phase. The various methods employed for the determination of rotational viscosities are then described in detail arid the experimental set up used in different cases are explained.

A comparison between the values obtained by the different methods is given. Results of the effect of alkyl chain length on the magnitude and temperature variation of γ_ϕ are presented. Finally the thermal variation of the soft mode viscosity γ_s in the A phase is discussed.

4.2 Rotational viscosity in the smectic C* phase

Consider first a nematic liquid crystal in which the director is rotating by the application of an electric or magnetic field rotating about Y-axis. The resistance of the system to such a rotation can be described by the torque equation[14]

$$\Gamma^n = -\gamma \frac{d\phi}{dt} \tag{4.1}$$

where Γ^n is tlic torque required to maintain an angular velocity $d\phi/dt$ arid γ is tlie associated rotational viscosity coefficient. ϕ is tlie angle the director makes with the initial director position as shown in Fig. 4.1.

The problem is more complicated in tlic smectic phase due to tlic presence of layering. Hut for tlie type of viscosities that we are interested in, a much simpler approach has been taken and a theory has been developed on the lines of the nematic viscosity coefficients. For this tlic major assumption that is made is that the

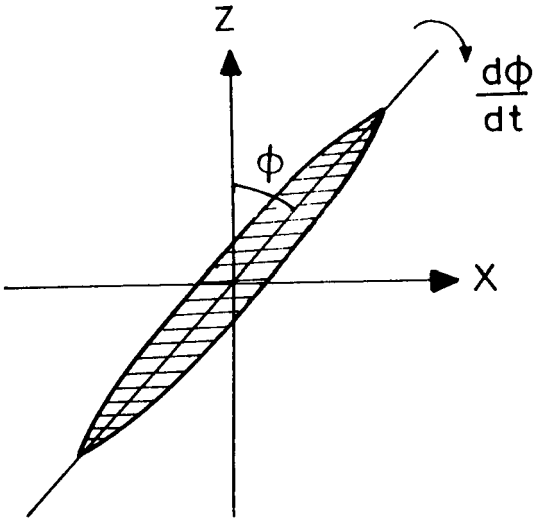

Fig.4.1. Director re-orientation in the nematic phase under the influence of a field.

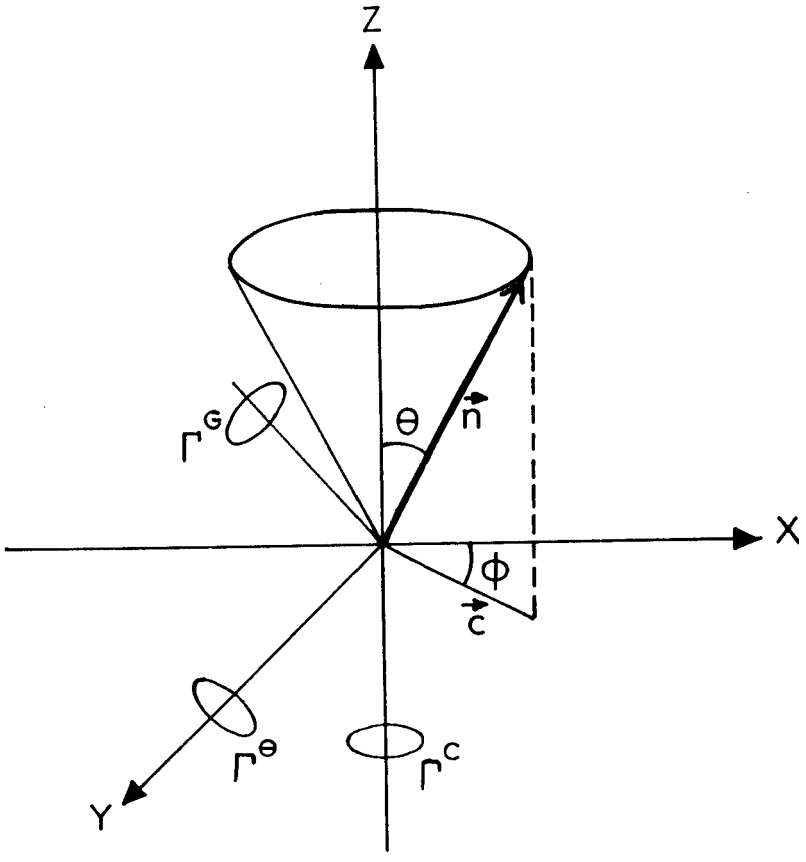

Fig.4.2. Definition of rotational viscosity coefficients in the smectic C* phase.

response of the system is purely confined to director rotation without any translational motion.

To define the rotational viscosity coefficients in smectic C* phase consider Fig. 4.2, where n is the director, 0 the tilt angle, $\boldsymbol{c}$ the in-plane smectic C director, ϕ its phase and xyz are the rectangular coordinates.

Just like in the nematic case, tlie viscous torque is given by

$$\Gamma = -\gamma \frac{d\phi}{dt} \tag{4.2}$$

where γ is a general viscosity coefficient. From tlie symmetry of tlie smectic C* phase it is clear that one of the principal axes of γ must he in the layer plane and perpendicular to the tilt direction. The corresponding torque is denoted by Γ_θ and the viscosity is γ_θ. γ_θ is tlie viscosity associated with the change in the magnitude of 0, and describes the tilt amplitude fluctuations. The transition between A and C* phases is second order or at most weakly first order. As such close to the transition a tilt fluctuation mode can be observed in tlie A phase. This mode softens on approaching tlie transition point. Therefore γ_θ is called tlie soft mode viscosity (γ_s). The second principal axis of γ is parallel to the director. This mode corresponds to the rotation of tlie molecule about its long molecular axis and the associated viscosity value is very small. The remaining principal axis must be in the tilt plane and perpendicular to the director **n** and the polarization P,. The corresponding viscosity is found to be similar to the nematic rotational viscosity and is denoted by γ_G. In the case of the C* phase the director **n** rotation is damped by a viscous force which is tlie z-component of tlie viscous torque acting on tlie director **n**. One can obtain an expression for this torque and hence for γ_G by considering eqn.(4.2), i.e.,

$$\Gamma^G = -\gamma_G \frac{\partial \phi}{\partial t} = -\gamma_G \mathbf{n} \frac{\partial \mathbf{n}}{\partial t} = -\mathbf{n}\gamma_G \dot{\mathbf{n}}$$

To find the value of $\dot{n}$ consider the components of $\mathbf{n}$ along x, y and z axes.

$$\begin{aligned} n_x &= n \sin\theta \cos\phi \quad \text{therefore } \dot{n}_x = -n\dot{\phi} \sin\theta \sin\phi \\ n_y &= n \sin\theta \sin\phi, \quad \dot{n}_y = n\dot{\phi} \sin\theta \cos\phi \\ n_z &= n \cos 0, \quad \dot{n}_z = 0 \end{aligned}$$

Therefore $\dot{\mathbf{n}} = \mathbf{n}\phi \sin\theta$

and

$$\Gamma^G = -\gamma_G \mathbf{n} \cdot \mathbf{n}\phi \sin\theta = -\gamma_G \phi \sin 8 \tag{4.3}$$

The z component of this torque is $\Gamma_z^G = \Gamma^G \times \sin 0$, i.e.,

$$\Gamma_,^G = -\gamma_G \sin\theta \times \dot{\phi} \text{ x } \sin\theta = -\gamma_G \sin^2\theta\dot{\phi} \tag{4.4}$$

Usually one introduces another viscous torque Γ_c for the rotation of the c-director about the layer normal, i.e., z-axis (see Fig.4.2). The corresponding viscosity is γ_ϕ associated with the rotation of **c**-director about z-axis which is similar to the rotation of the director **n** about the layer normal within the smectic cone. One can obtain an expression for γ_ϕ by considering the components of c-director and using the torque equation as

$$\Gamma_,^C = -\gamma_\phi \mathbf{c} \cdot \dot{\mathbf{c}} = -\gamma_\phi \phi \tag{4.5}$$

Comparing Eqs. (4.4) and (4.5)

$$\gamma_\phi = \gamma_G sin^2\theta \tag{4.6}$$

'Though γ_ϕ is the viscosity associated with the rotation of the director **n** about the layer normal, but it has been argued[10] that γ_G is the more fundamental rotational viscosity as it defines the rotation of **n** about an axis perpendicular to both **n** arid **P**, lying in tlie tilt plane. In contrast γ_ϕ is a derived quantity composed of γ_G and 0. Thus the temperature dependence of γ_ϕ not only involves the temperature dependence of γ_G hut also the temperature variation of 0. Further if one wants to compare P_s and rotational viscosity, it is γ_G which has to be considered and riot γ_ϕ, as P_s arid γ_ϕ comparison might include a mutual relation between P_s and θ.

As γ_G is related wit h the rotation of **n** about the layer normal, it is also called as the Goldstone mode rotational viscosity (in analogy with tlie symmetry recovering Goldstone mode studied in dielectrics, Chapter III). A pictorial representation of rotational viscosities, in nematic,SmA and SmC*, is given in Fig.4.3.

Rotational viscosity in smectic C* phase is measured by methods based on mechanical,[15] pyroelectric[5,16] and electrical[6–10] techniques. Tlie mechanical methods involve disturbance of tlie helix in the smectic C* phase by an alternating shear or Poisseuille flow which gives information on the viscoelastic coefficients. However, these methods are not commonly used because of tlie complicated experimental set up. The pyroelectric method has been successfully employed to determine both γ_s and γ_ϕ. In this method using a short laser pulse tlie liquid crystal layer is heated; due to this heating tlie director tilt changes arid thus the P_s reorients giving rise to an induced pyroelectric current. By studying this transient current decay, γ_s value can be obtained. This technique also needs a sophisticated set up. In tlie electrical method the rotational viscosities can be determined either (a) by studying the current[6–8] or optical[4] response to an applied alternating electric field or (b) by dielectric[9,10] measurements. We have employed tlie electrical method and used

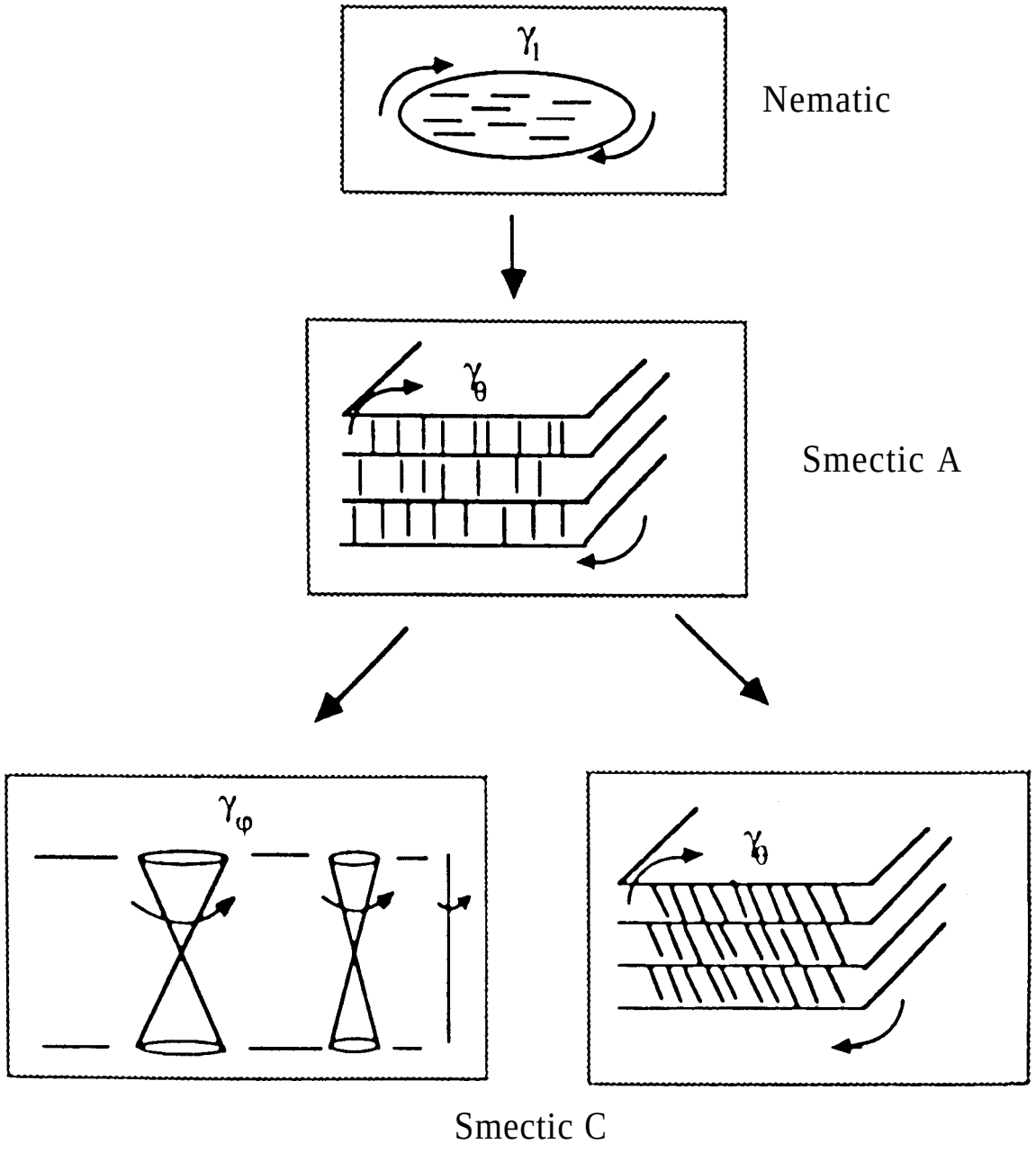

Fig.4.3. The single rotational viscosity in the nematic and smectic A phase will be split into two in the smectic C phase, associated with motion on tlie cone and tilt-angle variations, respectively. (From K. Skarp, Ref.3).

technique (a) for the measurement of γ_ϕ and technique (b) for determining γ_s. The principles involved and tlie experimental set up are described in detail below.

4.3 Electrical methods of measuring γ_ϕ

In this method γ_ϕ is usually determined in thin samples by applying an oscillating electric field and either measuring tlie time required for an optical transmittance change - the optical response method or by measuring the current induced due to reversal of the polarisation - the field reversal method. Usually optical transmission method is done using a square wave, whereas in the field reversal method one can employ a square wave or a triangular wave or a sine wave. Depending on tlie type of tlie input wave there are different field reversal methods for measuring γ_ϕ. All these methods are described in the following.

4.3.1 Optical response method

Here a low frequency square wave of sufficiently high amplitude is applied to a homogeneously aligned smectic C* sample and the temporal variation of the transmitted part of an incident polarised light is used as a measure for tlie calculation of tlie response time τ, and γ_ϕ is calculated using an empirical formula $\gamma_\phi = \tau P_s E$, where P_s is the spontaneous polarisation, E is the applied electric field.

To find τ consider an aligned smectic C* sample. Let all the dipoles he in the up state when tlie applied voltage is +V at any instant of time. When tlie direction of the applied voltage changes from +V to -V, tlic dipoles will rotate by an angle 20 and the dipoles will align in the down state. Because of tlie viscosity a definite time is needed for tlic dipoles to orient from $+P_s$ to $-P_s$ and this time is called the switching time τ. The optical switching time τ is defined as tlic measured response

time for a full reorientation of tlie optic axis. (Note that for display devices[17] τ is given as the time required for an optical transmittance change from 10% to 90% when the applied field polarity is reversed. However we have considered tlie full switching time, i.e., the time for optical transmittance change from 0 to 100 % .) A typical optical response curve is shown in Fig. 4.4. With this measured value of τ one can calculate γ_ϕ using the relation

$$\gamma_\phi = \tau P_s E \tag{4.7}$$

4.3.2 Field reversal method

The basis of these methods is that when the polarity of a driving electric field is reversed a transient current is induced clue to tlie reorientation of the dipoles. This current contains tlie information about the dynamics of the polarization reversal and thus about the rotational viscosity. The expressions used to determine γ_ϕ depend on the shape of the applied field.

Field reversal using square wave field

The first attempt to measure γ_ϕ by this method was done by Skarp *etal.*,[6] The response time τ was defined as the time between the square wave pulse edge arid tlie peak position of tlie transient current. γ_ϕ was evaluated using the relation, $\tau = \gamma_\phi/(P_s E)$. Later Kimura *etal.*,[18] utilising the equation given by Xue-Jie *etal.*[19], introduced a correction factor and τ is given by $\tau = \tau_\omega/1.76$, where τ_ω is tlie full width at half maxima (FWHM) of the current peak. Now several simplified analytic switching models[19–22] exist enabling the evaluation of γ_ϕ from the polarisation reversal current. These models include considerations of tlie elastic (boundary) effects,[20] dielectric torque,[19] fluctuations[21] and layer tilt.[22] Of these models the model in which

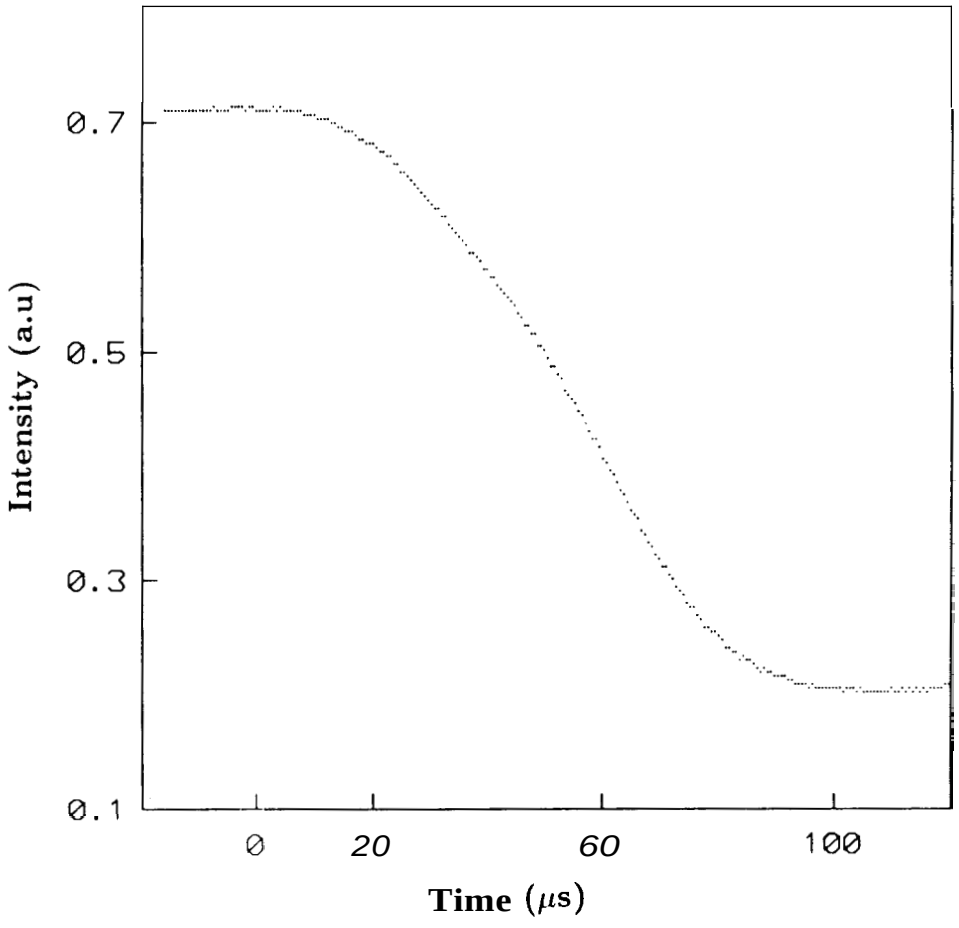

Fig.4.4. Optical response curve

elastic forces are considered predicts properly the position of the peak on the time axis and it also accounts for the sample alignment and thus one can determine γ_ϕ fairly accurately. Therefore we have adopted this model for the analysis of our field reversal current peak data.

In this model,[20] the flexoelectric effect and the effect of variation in the dielectric constant during the polarization reversal are neglected. The elastic torque is defined in such a way that it is 0 for $\phi = \pi/2$, (where ϕ is the angle between the electrode normal and the direction of P_s see Fig.4.5) which corresponds to the uniform orientation of P_s and it is non-zero for $\phi = 0$ and κ. Such an elastic torque can be assumed to be proportional to cos ϕ as for $\phi = \pi/2$, cos $\phi = 0$ and for $\phi = 0$ and π, cos ϕ is lion-zero. γ_ϕ, tlie viscosity which opposes tlie reorientation of the P_s in an alternating electric field is assumed to he proportional to $\partial\phi/\partial t$. Thus one can write the torque equation for equilibrium as

$$-PE \sin \phi + K \cos \phi = \gamma_\phi \frac{\partial \phi}{\partial t} \tag{4.8}$$

where K is an effective elastic constant.

By solving this equation one can get a relation for γ_ϕ as[20]

$$\gamma_\phi = \frac{PE}{\kappa cos\phi_0} \tag{4.9}$$

where

$$\kappa = \frac{1.76275}{\tau} \quad and \quad \tau = \tau_+ + \tau_-$$
$$\phi_0 = 2\sin^{-1}\left[\frac{\beta - (\beta^2 - 2\beta + 2)^{1/2}}{2(\beta - 1)}\right]$$

where $\beta = \exp(\kappa\tau_s)$.

The terms τ_s, τ_+ arid τ_- are defined in Fig. 4.6. Using tlie same parameters one can

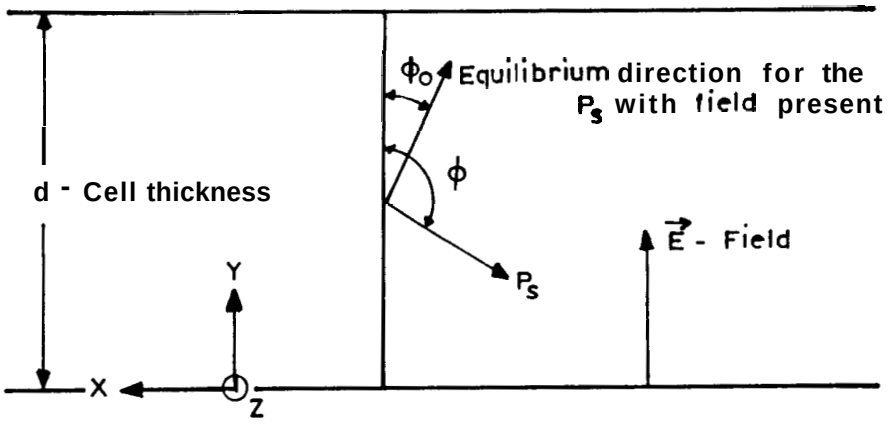

Fig.4.5. Geometry of the cell defining parameters used to derive eqn. (3.9). (After Dahl et al., Ref.20).

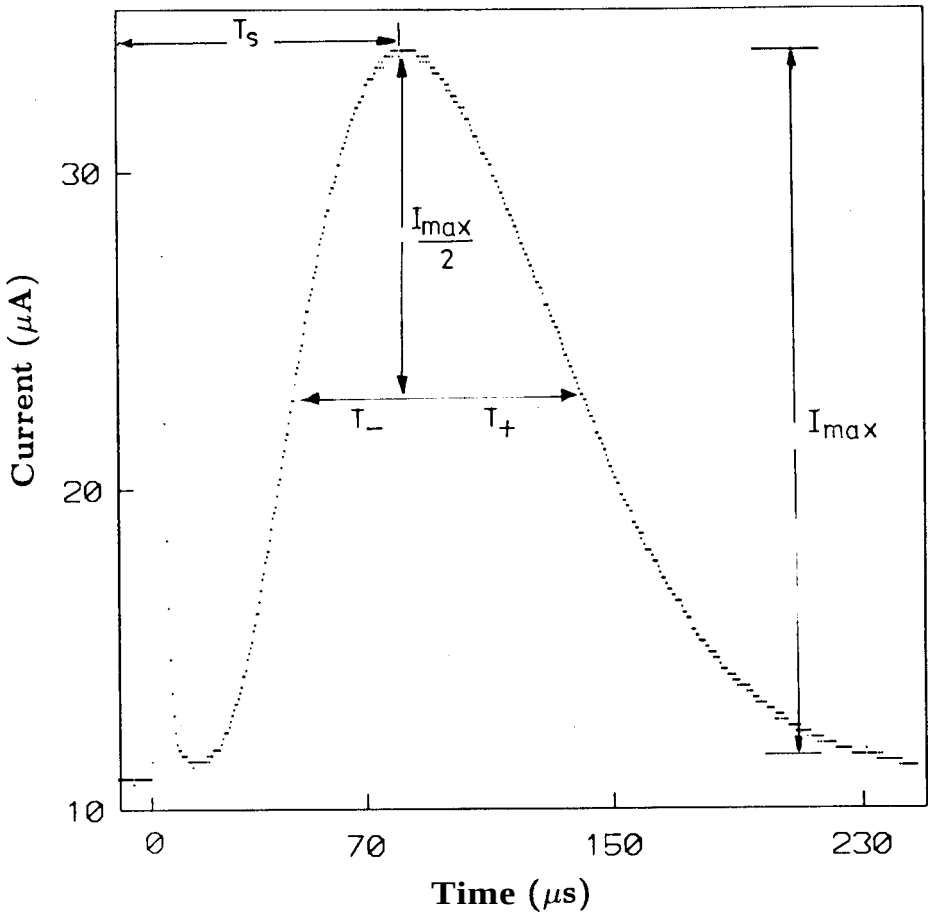

Fig.4.6. Current response to an applied square wave field experimental curve for D_8.

obtain an expression for the elastic constant K

$$K = P_s \, E \tan \phi_0$$

Field reversal using triangular wave field

To extract information about γ_ϕ from tlie transient current due to an applied triangular wave field we have adopted tlie model given by Escher *et al.*,[7] In this model tlie thermal fluctuations and interactions with tlie walls enclosing the liquid crystal arc not considered.

Consider an uniformly aligned C* sample. Let **n** be the director and θ the tilt angle between 11 arid layer normal z-axis. Let xz be the substrate plane (see Fig. 4.7). When a field E is applied along y-direction the P_s couples with the field and a torque E **e,** x **P,** is set which rotates tlie molecule about the z-direction and this rotation is opposed by tlie viscosity.

The torque balance equation is

$$\dot{\mathbf{L}} + \gamma_\phi \frac{\partial \alpha}{\partial t} + \mathbf{P}_{tot} \times \mathbf{E}_y = 0 \tag{4.10}$$

where L is the time derivative of the angular momentum I,, which comes due to the moment of inertia of the molecules. As L is small it can be neglected.

$$\gamma_\phi \frac{\partial \alpha}{\partial t} + \mathbf{P}_{tot} \times \mathbf{E}\mathbf{e}_y = 0 \tag{4.11}$$

Here $\mathbf{e}_y$ is the unit vector along tlic y-axis. P_{tot} is the total (spontaneous+induced) electric polarization. Since the magnitude of tlie applied field is not large, P_{tot} is approximated by P_s.

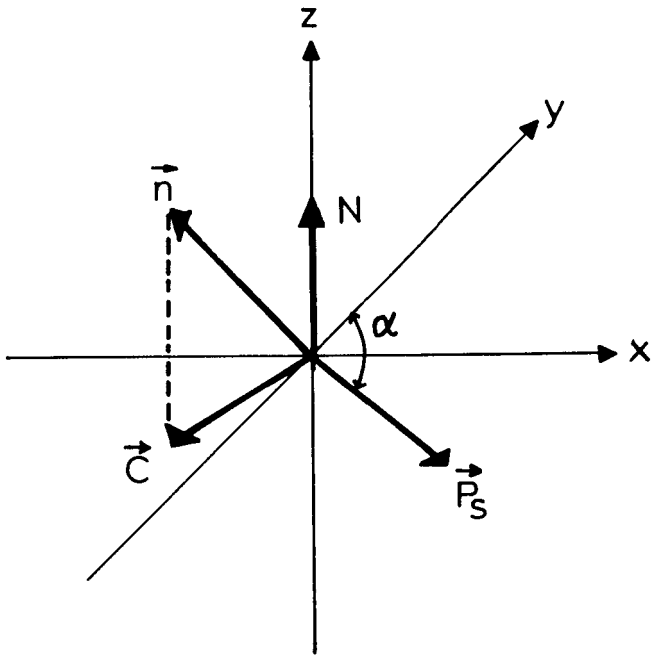

N - Normal to Smectic layer

$\vec{P}$ - Polarization

$\vec{C}$ - C - director

$\vec{n}$ - Director

Fig.4.7. C* structure showing $\vec{n}$, $\vec{P}_s$ and $\vec{C}$

Hence

$$\gamma_\phi \frac{\partial \alpha}{\partial t} + P_s \mathbf{x}\, \mathbf{Ee}, = 0 \tag{4.12}$$

$$\gamma_\phi \frac{\partial \alpha}{\partial t} + P_s E \sin \alpha = 0 \text{ or } \frac{\partial \alpha}{\partial t} = -\frac{P_s E \sin \alpha}{\gamma_\phi} \tag{4.13}$$

As both E and α are functions of time t,

$$\frac{\partial \alpha}{\partial t} = -\frac{P_s E(t) \sin \alpha(t)}{\gamma_\phi}$$

If **J** is the current density due to this spontaneous polarisation P_s one can write

$$J\mathbf{e}_y = \frac{\partial P_s . \mathbf{e}_y}{\partial t}$$

as $P_s = P_s \cos a\, e_y$ in the field direction

$$\mathbf{J} = -P_s \sin \alpha(t) \frac{\partial \alpha}{\partial t}$$

Putting value of $\frac{\partial \alpha}{\partial t}$ we get

$$J = \frac{-P_s sin\alpha(t)(-P_s E(t) sin\alpha(t))}{\gamma_\phi}$$

$$J = \frac{P_s^2 sin^2\alpha(t) E(t)}{\gamma_\phi}$$

According to Escher *et al.*,[7] for the determination of γ_ϕ, it is sufficient to find J_{max}, the maximum value of J. It is given by

$$J_{max} = \frac{P_s^2 E_{max}}{\gamma_\phi}$$

But $J_{max} = I_{max}/A$, where A is tlie active area of tlie electrode.

Hence

$$\frac{I_{max}}{A} = \frac{P_s^2 E_{max}}{\gamma_\phi} \tag{4.14}$$

$$\gamma_\phi = \frac{A P_s^2 E_{max}}{I_{max}} \tag{4.15}$$

The output wave of the forni shown in Fig. 4.8 gives the value of maximum current I_{max} and the corresponding electric field E_{max} is taken from the input field at that instant.

Transient current response to an applied sine wave field (The hysteresis loop method)

The method is based on the well known Sawyer-Tower method[23] or the hysteresis loop method, which was modified by Diamant et *al.*,[24] Tlie details of this method are already given in chapter II. Now we explain how γ_ϕ can be determined by the hysteresis loop method.[8]

Consider tlie Diamant bridge circuit shown in Fig. 4.9. When a sine wave $U_x = U_o \sin \omega t$ is applied to the sample a hysteresis loop as shown in Fig. 4.10 is obtained. Tlie amplitude of the output voltage U_y developed across the capacitor C (C=C_f of Fig. 4.9) gives the value of P_s. [Note that, when the bridge is balanced, tlie linear electric elements like ionic and capacitive induced currents arc balanced by the compensating resistor R_C arid capacitor C_C.]

If A is tlie active electrode area then

$$P_s = \frac{C U_y}{A} \tag{4.16}$$

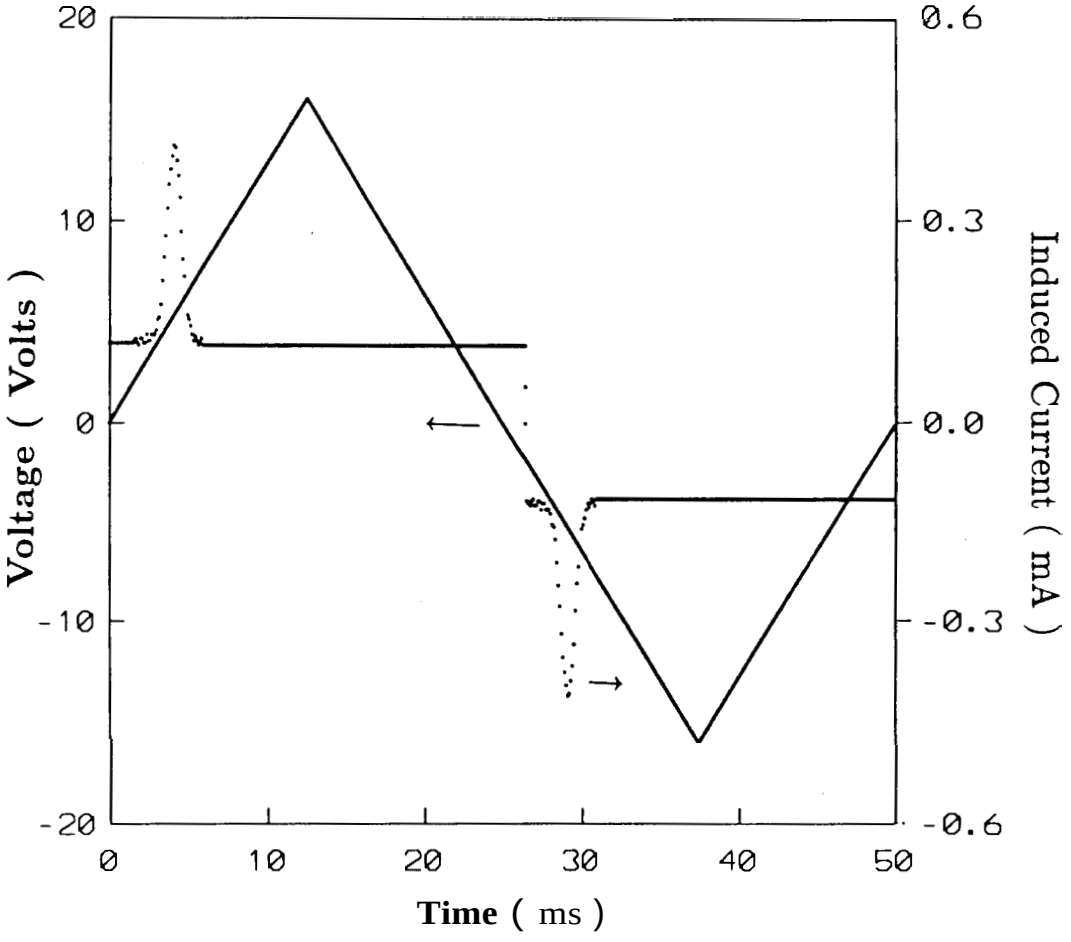

Fig.4.8. Current response to an applied triangular wave field - experimental curve for D_8.

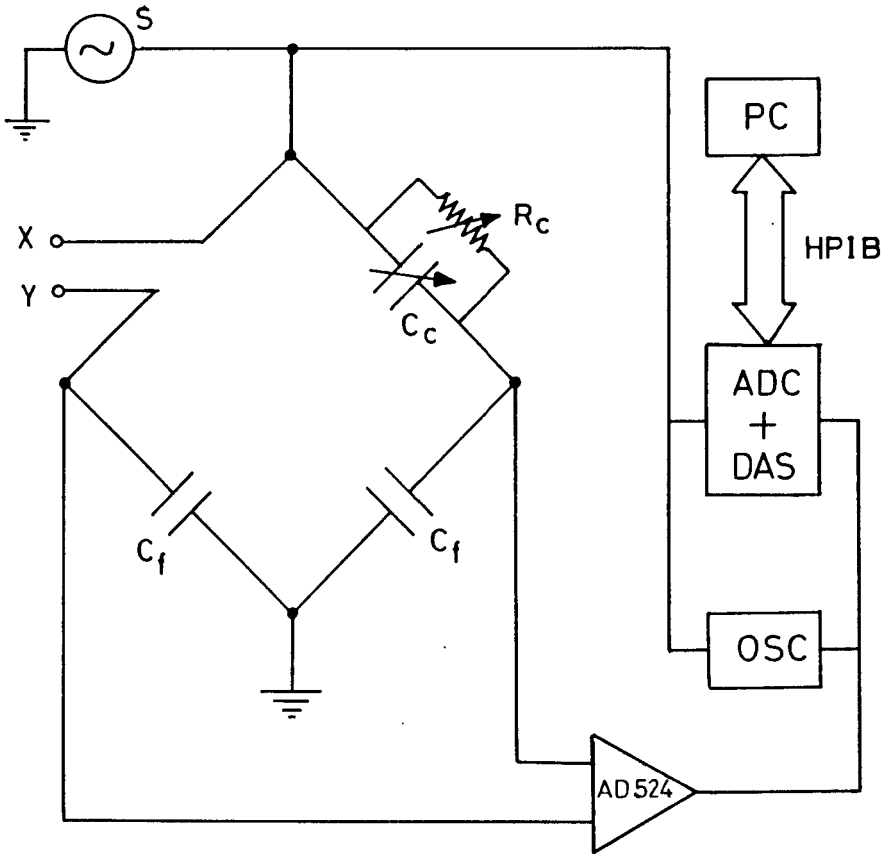

Fig.4.9. (a) Experimental set-up on Diamant bridge technique. S: Signal source; X,Y : Sample leads; R_s, C_c : Compensating resistor, Capacitor combination; C_f : Fixed capacitor; OSC : Dual channel storage oscilloscope; ADC + DAS : Analog-Digital Converter and Data Acquisition System; PC : Personal Computer. AD524 is a programmable gain instrumentation operational amplifier.

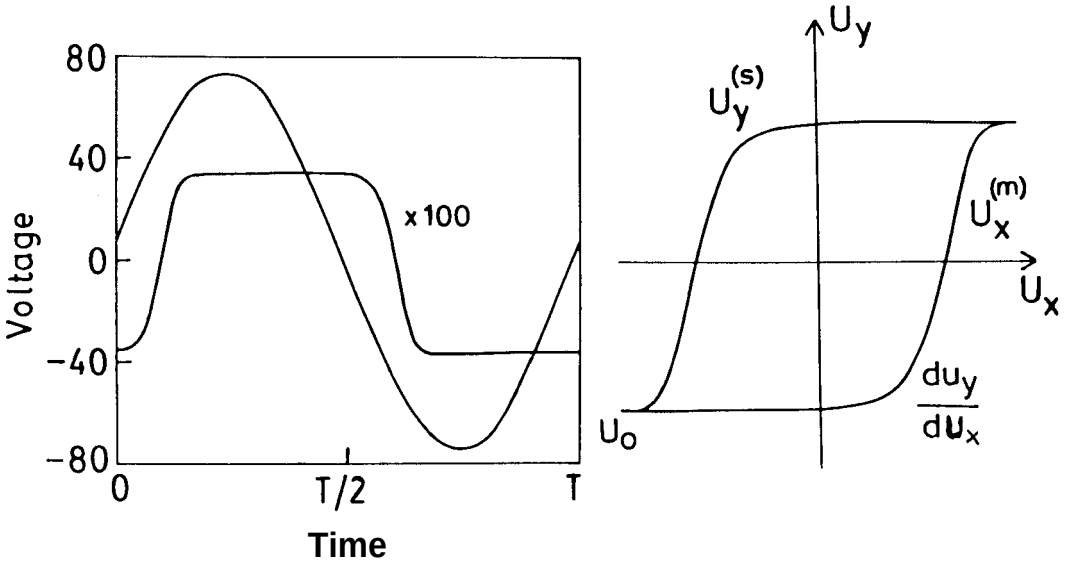

Fig.4.10. Current response to an applied sine wave field and the hysteresis loop - experimental curve for D_8.

[Note that U_y is. tlie maximum of tlie output as tlie applied field goes through a cycle.] These parameters can be used in the following way to obtain γ_ϕ using tlie relation **(4.15).**

If $J_{,,}$ is the maximum current density, then $I_{,,} = A\ J_{,,}$

Also $J_{,,} = \frac{\partial P_s}{at.} - \frac{a}{at}\frac{CU_y}{A} - \frac{C}{A}\frac{\partial U_y}{at}$

But $\frac{\partial U_y}{\partial t} = \frac{\partial U_y}{\partial U_x} \times \frac{\partial U_x}{\partial t}$

Substituting for U_x,

$$\frac{\partial U_x}{at} = w\, U_o \cos wt$$

or

$$J_m = \frac{C}{A}\frac{\partial U_y}{\partial U_x}\omega\, U_o \cos \omega t$$

or

$$I_m = AJ_m = C\omega U_o \cos wt \frac{\partial U_y}{\partial U_x} \tag{4.17}$$

Since $U_x = U_o \sin wt$

$$\frac{U_x^2}{U_o^2} = \sin^2 wt = 1 - \cos^2 wt$$

$$cos\,\omega t = \frac{(U_o^2 - U_x^2)^{1/2}}{U_o}$$

Therefore the maximum current $I_{,,}$ is given by

$$I_{,,} = C\omega U_o \frac{(U_o^2 - U_x^2)^{1/2}}{U_o}\frac{\partial U_y}{\partial U_x} \tag{4.18}$$

Putting this in eqn. (4.15) we get

$$\gamma_\phi = \frac{AP_s^2 E_m}{C\omega(U_o^2 - U_x^2)^{1/2}\frac{\partial U_y}{\partial U_x}} \tag{4.19}$$

But $P_s^2 = \frac{C^2 U_y^2}{A^2}$ and $E_m = \frac{U_x^m}{d}$,

where d is the thickness of the cell.

Hence

$$\gamma_\phi = \frac{C^2 U_y^2}{A}\ \frac{U_x^m}{d}\ \frac{1}{C\omega(U_o^2 - U_x^2)^{1/2}\frac{\partial U_y}{\partial U_x}}$$

or

$$\gamma_\phi = \frac{CU_y^2 U_x^m}{A\omega d(U_o^2 - U_x^2)^{1/2}\frac{\partial U_y}{\partial U_x}} \tag{4.20}$$

Thus γ_ϕ is expressed in terms of the known parameters of the hysteresis loop as shown in Fig. 4.10. Here $U_x^m = U_x$ at $U_y = 0$ and U_y is the maximum value of U_y. From the liysteresis loop one can get the values of U_y, U_x at $U_y = 0$, $\frac{dU_y}{dU_x}$ and the amplitude of the applied field, U_o and hence γ_ϕ can be determined. An advantage of this method over the polarisation reversal methods is that the contribution coming from the linear electric elements is eliminated by the balance condition of the bridge. A more appealing advantage is that in the same experiment one can simultaneously determine P_s, γ_ϕ and the coercive field E,.

4.4 Materials

Measurements were done on six homologs (n = 7 to 12) of the series [2S,3S]-4′-(2-chloro-3-methylpentanoyloxy)phenyl *trans*-4″-n-alkoxy cinnamates.[25] The structural formula and transition temperatures in ("C) for these compounds (short form D_n)

are already given in Table 2.1. The reason for choosing this series of compounds is that, as already observed in chapter II, the P_s value of these compounds is high and the temperature range of smectic C* phase is also large for all the homologs. Further the critical field, necessary for unwinding tlie helix, is small ($\approx$ **10** kV/cm) for all the homologs even at T_c – T = 10^oC.

4.5 Experimental

4.5.1 Preparation of the sample cell and alignment

The preparation of the sample cell and the method employed for obtaining good sample alignment have already been described in chapter II. During any measurement tlie temperature of the cell was kept constant to bettcr than $\pm 5mK$.

The different experimental set-ups used for the measurement of γ_ϕ are described below.

4.5.2 Optical transmission method

The experimental set up used for this experiment is shown in figure **4.11.** A homogeneously well aligned sample cell is placed between a polariser and an analyser. A He-Ne laser (Spectra Physics 120S) with a low amplitude drift was used as the source. The transmitted intensity was detected with a fast response (rise time $\sim$ **10** ns) and low dark current photodiode (Centronics OSI5). A square wave pulse applied to the sample switches the director by an angle 20 (θ being the tilt angle) when its polarity is reversed. The output of the photodiode and the applied square wave signal were fed to a storage oscilloscope (Philips PM2203) which was triggered by the positive leading edge of the applied signal. The data acquired was then transferred to a microcomputer for storage and analysis. By setting tlie polariser and

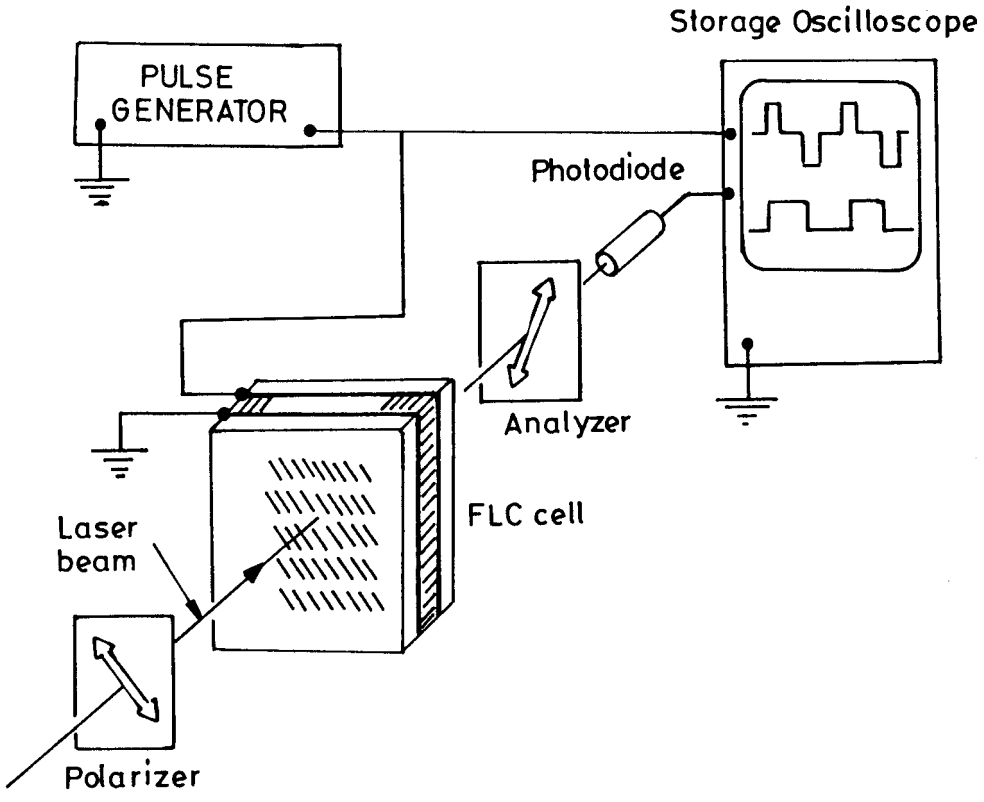

Fig.4.11. Set-up for optical response time measurements.

analyser properly perfect light modulation can be obtained from which the exact switching time can be determined. A typical response curve is shown in the figure 4.4. Since our interest is to compare optical and non optical methods of obtaining γ_ϕ values,we took the 0-100% intensity variation time as tlie switching time τ rather than the usually used 10-90% time.

4.5.3 Transient current response to an applied square wave field

The experimental set up used is shown in figure 4.12. The function generator used (HP 8116) could deliver a maximum amplitude 32 V peak to peak (which was sufficient to generate fields as high as ≈30 kV/cm). The square wave field when applied to tlie sample causes a reversal of tlie dipoles when its polarity is reversed. The current associated with this reversal is measured as a voltage drop across tlie current sensor resistor R_s connected in series with tlie sample. The value of R_s should he carefully selected such that it makes a negligible contribution to tlie RC time constant of the cell. The output and input signals were fed to a dual channel storage oscilloscope PM 2203. The data acquisition and control was handled by a microcomputer. Fig. 4.6 is a typical field reversal current peak in which different parameters involved in the calculations of γ_ϕ are defined.

4.5.4 Transient current response to an applied triangular wave field

Basically the experimental set up and the data acquisition process arc similar to the square wave method. The input wave and the sample response are shown in fig. 4.8. By finding the maximum current I_{max} and the corresponding applied field E_m, the value of γ_ϕ was evaluated.

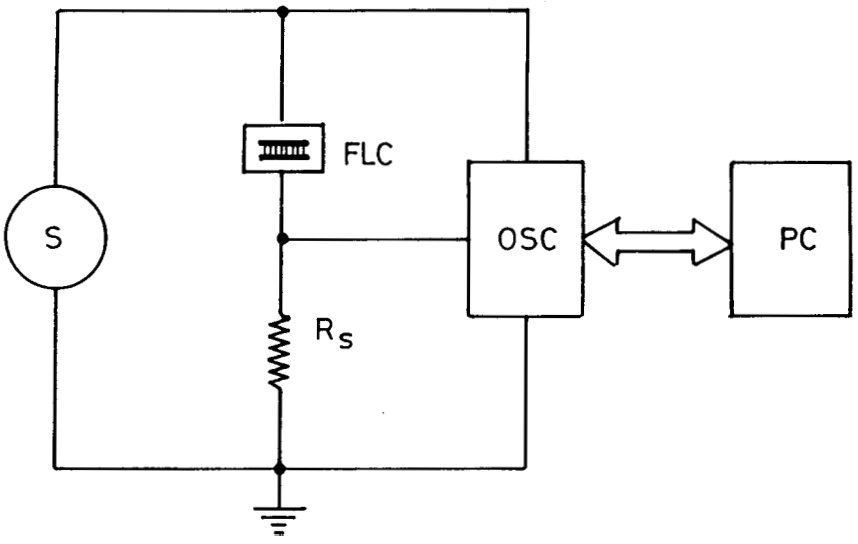

S - Signal source

FLC - Ferroelectric Liquid Crystal Sample cell

R_S - Current sensor resistor

OSC - Dual channel memory oscilloscope

PC - Personal Computer

Fig.4.12. Block diagram for the field reversal techniques.

4.5.5 Hysteresis loop method

For this method a calibrated Diamant bridge (described earlier in chapter II) was used to obtain the D-E hysteresis loop of the sample due to an applied sine wave field. By adjusting tlie value of tlie resistor R_C and capacitor C_C one can cornpensate for tlie ionic and capacitive contributions and obtain a hysteresis loop as shown in the Fig. 4.10. The data acquisition and analysis were handled by a high resolution data acquisition system (HP7090A) and a computer as explained in chapter II. With the help of tlie hysteresis loop it is possible to obtain the different parameters needed to calculate γ_ϕ as defined in the Fig. 4.10.

4.6 Results and Discussion

4.6.1 Comparison of γ_ϕ values obtained by different techniques

Figure 4.13 is an arrhenius plot of $ln\,\gamma_\phi$ vs. $1/T$ for tlie 8th homolog of the D_n series. Here we have plotted tlie γ_ϕ values obtained by tlie four different methods described above. It is clearly seen that throughout the range of the measurement there is excellent agreement between the γ_ϕ values determined from tlie different techniques. Further it is seen that except close to the A - C* transition temperature T_{AC*} the behaviour is of Arrhenius type. Thus the temperature variation of γ_ϕ can be expressed as $\gamma_\phi = \gamma_{\phi_o} e^{\mu/kT}$, where μ is the activation energy. The value of μ obtained by fitting tlie data away from T_{AC*} to the above equation is μ =1.62 eV. Close to the transition the behaviour is non-Arrhenius and a power law type of expression may describe the data better than the Arrhenius law. However, a single exponent does not seem to describe the data over a wide range of temperature. This may probably be due to the mean field to tricritical cross-over behaviour[26] generally

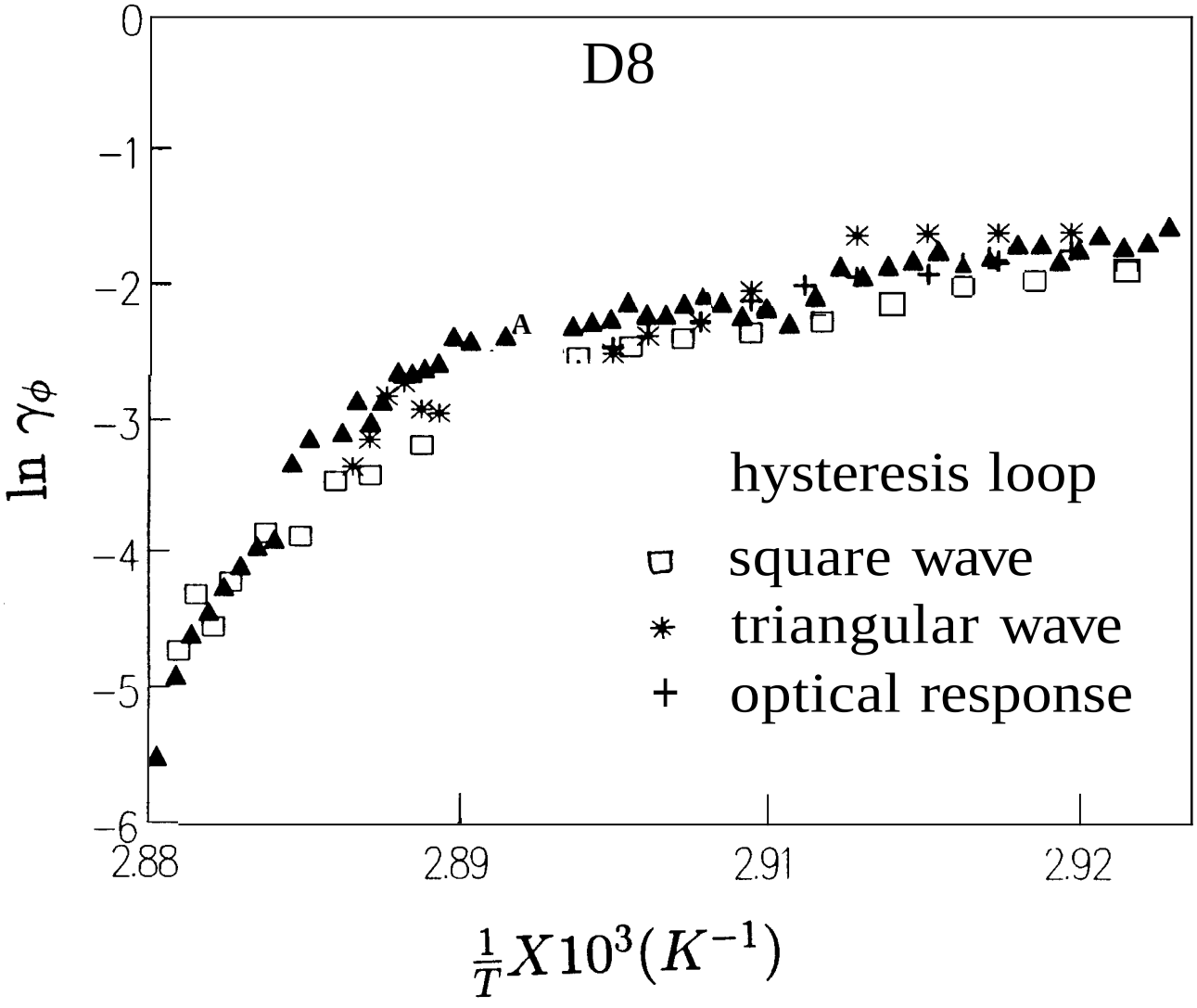

Fig.4.13. Comparative plot of $ln\gamma_\phi$ versus $1/T$ for D_8 obtained by four techniques discussed in the text.

observed near tlic A-C* transition.

4.6.2 Effect of Chain Length

In Fig. 4.14 we have plotted $ln\gamma_\phi$ as a function of 1/T for the six homologs of the series (n = 7 to 12). In this plot we present only the results obtained using the hysteresis loop method which, as we showed in the previous section, agree very well with tlic values determined by the other methods. The reasons for choosing the hysteresis loop method are following: (1) The advantage of using tlie hysteresis loop method as compared to the polarization reversal method is that the background current coming from the linear electric elements need not be taken into account or substractecl numerically which pose inconvenience in the exact determination of γ_ϕ. In the hysteresis loop method these linear electric elements are eliminated by the balance condition of the bridge. (2) In the same run one can collect tlie information about P_s and γ_ϕ. In Fig.4.14 we have normalised the plots by assuming a single T_c to facilitate comparison between different homologs. The notable features are (1) there is a systematic variation of γ_ϕ with chain length. (2) Similar to the 8th homolog, tlie overall variation of tlie γ_ϕ appears to be of power law type. But if the data away from the T_c is considered it appears to follow Arrhenius law. It is clear from the Fig.4.14 that away from the transition the slope of the plots and hence tlie activation energy is approximately the same for all tlie hornologs, showing thereby that all hough tlic absolute value of γ_ϕ is very much influenced by the chain length, its temperature variation is the same for all the homologs. This perhaps suggests that tlie alkyl chain length is responsible only for the absolute value of γ_ϕ whereas its temperature variation is independent of n and controlled hy the rigid core. Fig.4.15 shows γ_ϕ (at $T_c - 5^oC$) as a function of chain length for all the homologs n=7 to 12. From the figure it is seen that γ_ϕ decreases rapidly with n for lower homologs and

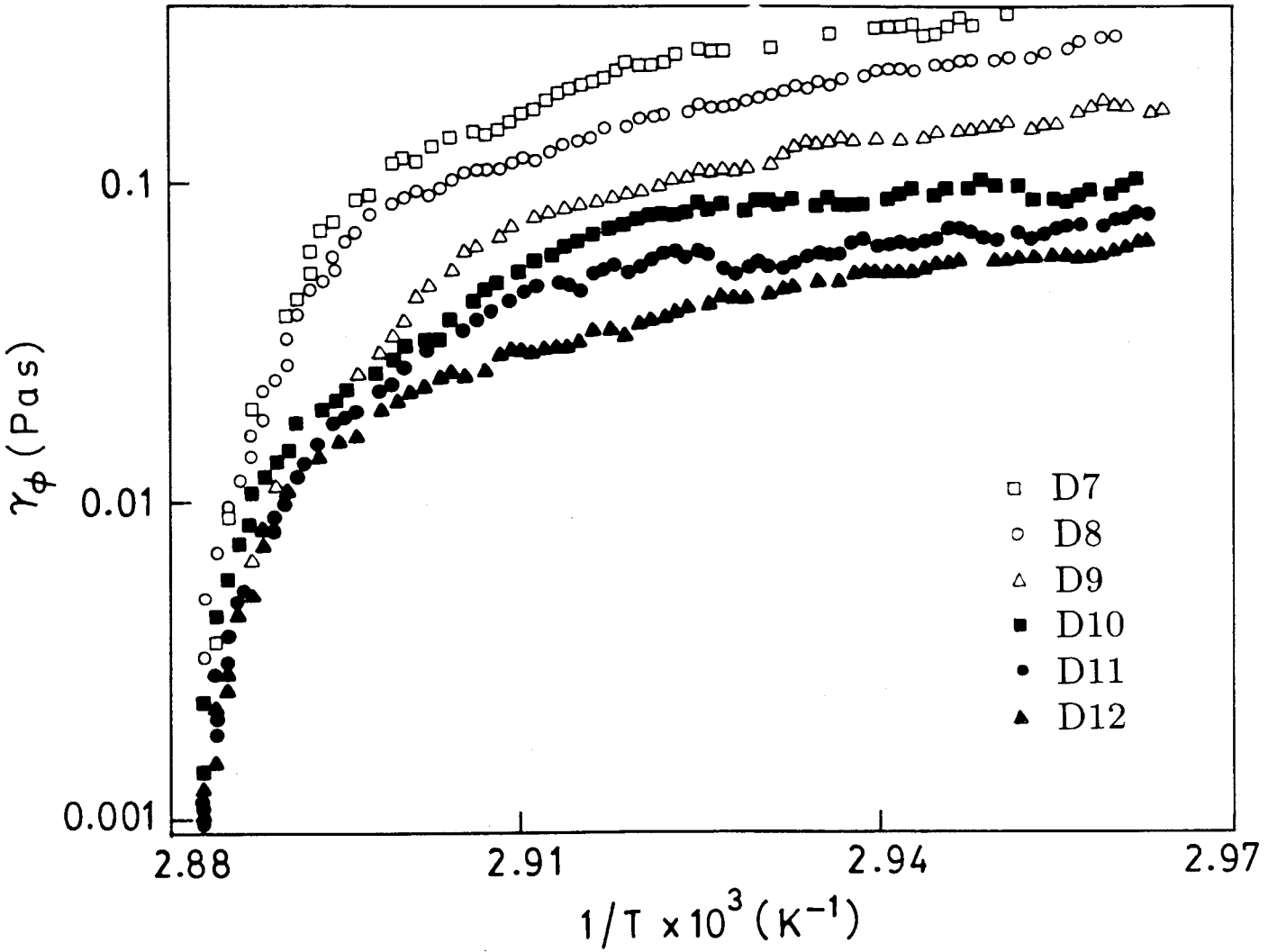

Fig.4.14. Plot of $ln\gamma_\phi$ versus $1/T$ for the six homologs D_7 to D_{12}.

but appears to reach a lower limit and stabilize for longer chain lengths. However, the P_s variation with n is different in that it varies linearly with n as seen from the Fig.4.16. Using tlie relation $\tau = \gamma_\phi / P_s E$ we have calculatecl for all the homologs the value of τ at $T_c - 5^oC$ at an applied field value of 50 kV/cm. The plot of τ vs. n is shown in Fig. 4.17. It is clear from tlie figure that τ is very much sensitive to the chain length for lower homologs and it reaches a limiting value for the higher homologs. The limiting value may perhaps be imposed by the rigid core. This suggests that while selecting materials for fast response tlic limitation imposed by the rigicl core should also be kept in mind.

In order to study the effectof subtle changes in the molecular structure on the value of rotational viscosity γ_ϕ and tlic rise time τ we have measured the γ_ϕ and τ for 10th homologs of the four series which have almost similar molecular structure (series A,B,C and D) discussed in Chapter II. In Figs. 4.18a-4.18d, we have plotted τ vs $(T_c - T)$ for the 10th homolog of the four series obtained with a field of 30 kV/cm. The figures show tliat in all the four series τ varies in a non-linear fashion as tlie temperature is changed. The variation of τ is steeper in series A and B compared to series C and D. Comparing the values obtained at $T_c - \mathrm{T} = 5^oC$ we see that series D has the smallest value $\simeq 25\mu sec$ and series C has 45 μsec whereas series A and B have the same value $\simeq 60\mu sec$. Thus one can probably conclude that in order to reduce the switching time it is better to cluster tlie chiral groups together and attach them directly to the core. This also happens to be tlic criterion for getting higher polarization values as we have seen in Chapter II.

Figures 4.19a-4.19d show the plots of γ_ϕ and γ_G=$\gamma_\phi / \sin^2 \theta$ as a function of temperature for the 10th homolog of tlic each series calculated at a field of 30 kV/cm. It is seen that the values of γ_ϕ and γ_G are not very different for the four

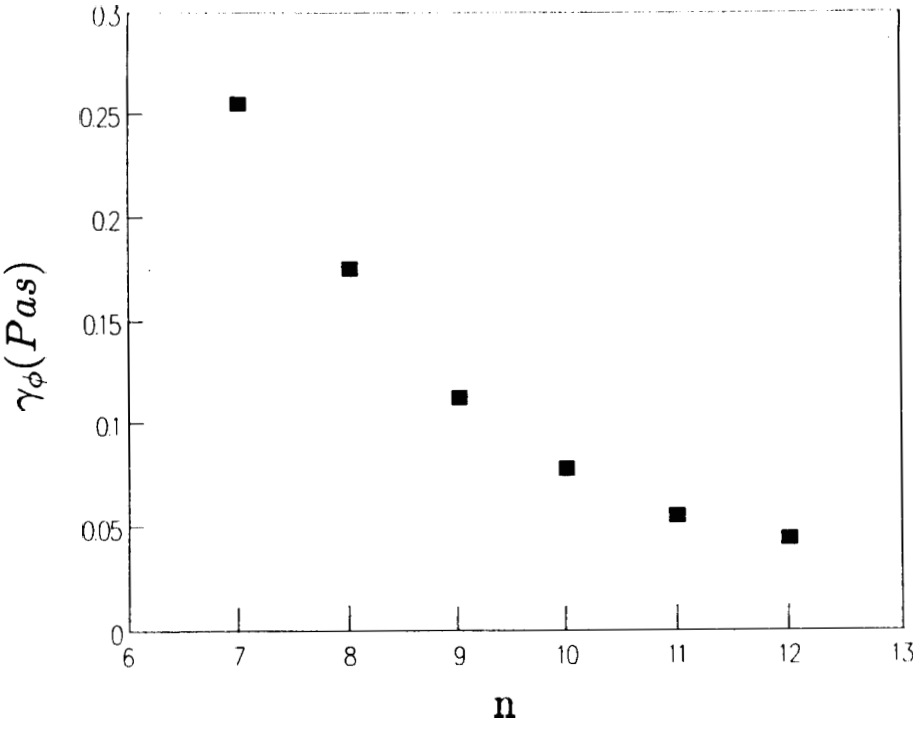

Fig.4.15. Dependence of γ_ϕ on chain length at $T_c - 5°C$.

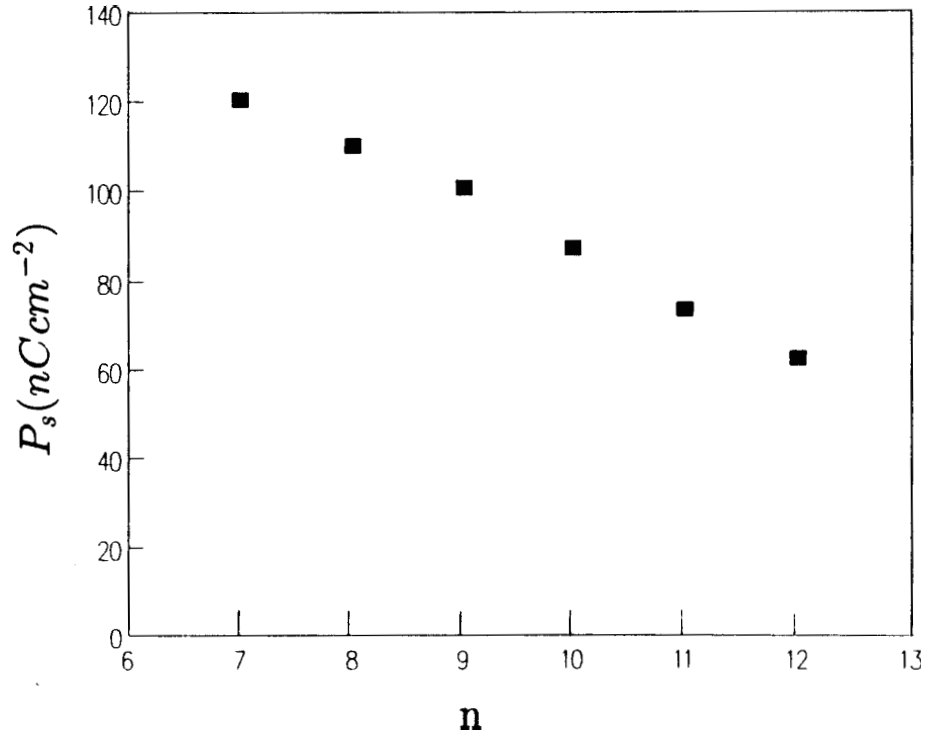

Fig.4.16. Dependence of P_s on chain length at $T_c - 5°C$.

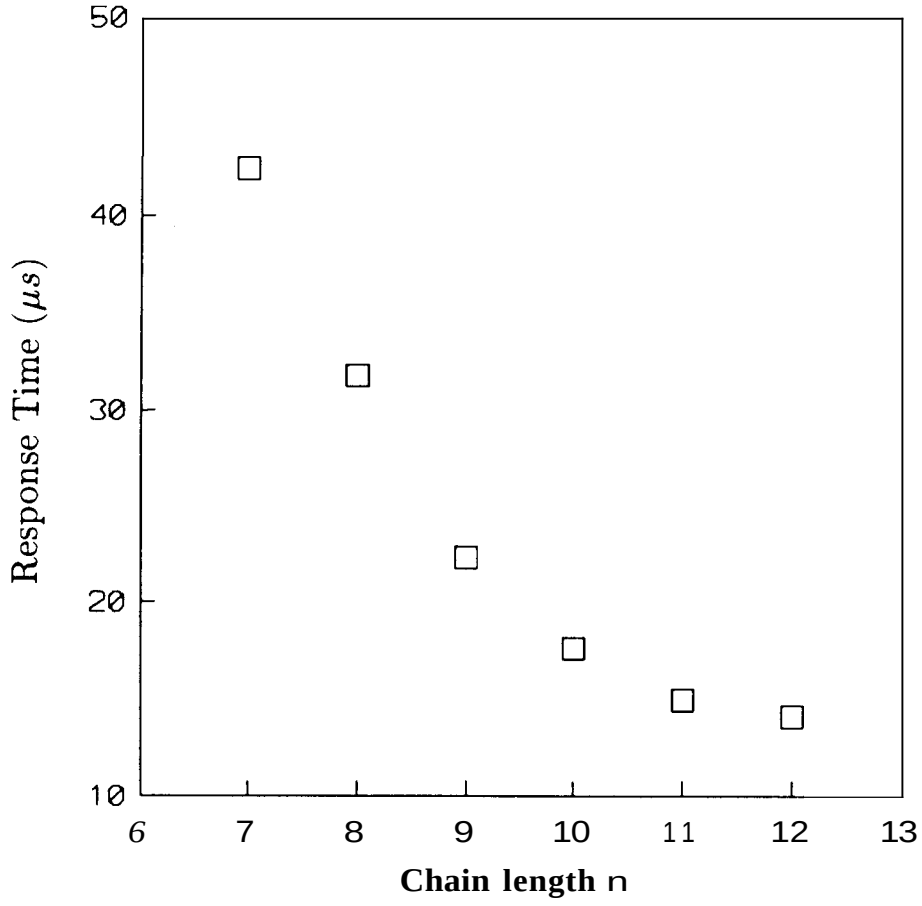

Fig.4.17. Dependence of response time τ on chain length at $T_c - 5^oC$.

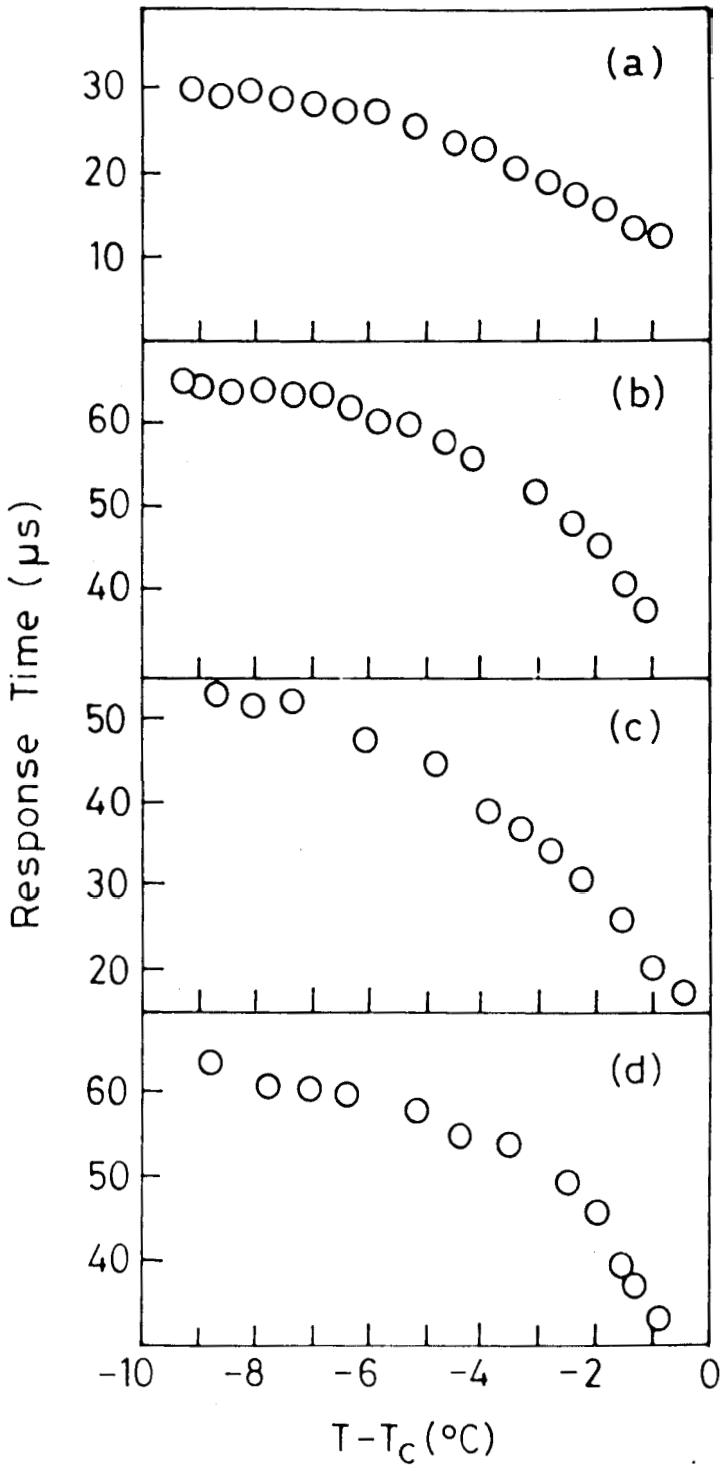

Fig.4.18. Response time as a function of temperature for n = 10 of (a) series D_n, (b) series B_n, (c) series C_n and (d) series A_n.

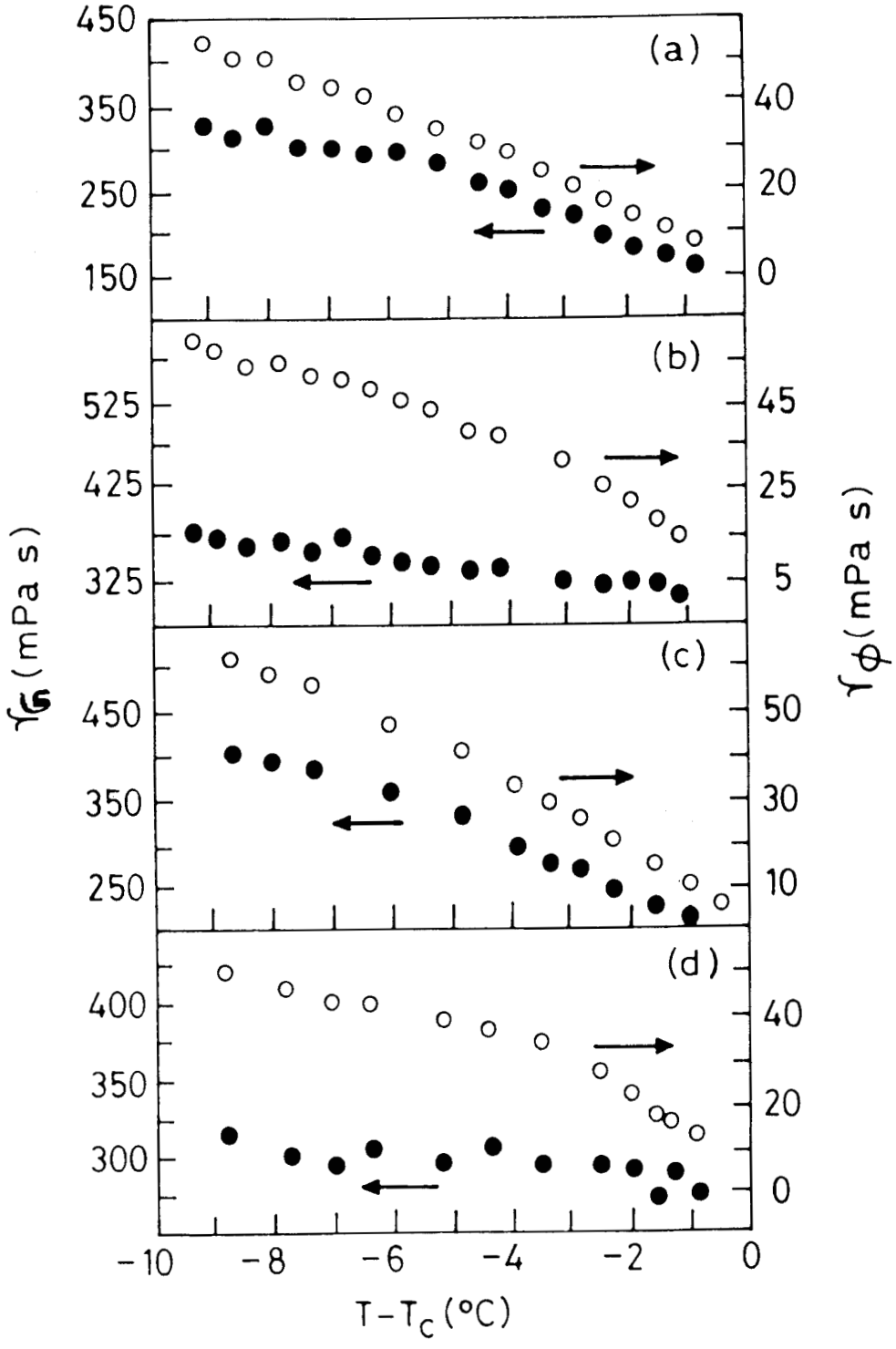

Fig.4.19. Rotational riscositirs γ_{G_1} and γ_ϕ versus temperature for n = 10 of (a) series I)„ (b) series B_n, (c) series C_n and (d) series A„.

compounds, e.g., at $T_c - 5^oC$, $\gamma_\phi \approx 40mPaS$. However tlie variation of γ_G with temperature is different for series A arid B. For series A and B the γ_G variation is very small with temperature. This confirms the statement made earlier that γ_G is the true rotational viscosity and one has to take γ_G and not γ_ϕ while considering the temperature variation of the rotational viscosity. (In fact, as we shall see later in Fig.4.24, tlie data collected at close intervals of temperatures brings out this feature beautifully.) However for series C and D γ_G varies initially and appears to attain a steady value at lower temperatures.

In order to do a quantitative comparison of the effect of P_s on γ_ϕ we have calculated a quantity P_s/γ_ϕ which is the inverse of tlie product τE; tlie greater the value of P_s/γ_ϕ the better will be the switching. In table 4.1 we have tabulated P_s/γ_ϕ for n = 10 of each series. The table sliows that series D, having 2 chiral groups near the core, has the highest value of P_s/γ_ϕ. The value P_s/γ_ϕ = 0.025 C/m^{2}PaS for n = 10 of series D compares fairly well with the values reported by Otterholm et *al.*,[27] and Chandani *et al.*,[28] (0.04 and 0.06 C/m^{2}PaS respectively).

4.6.3 Soft Mode Viscosity γ_s

Unlike γ_ϕ, there are only a few studies[5,9] of y,, the viscosity associated with tilt amplitude fluctuations. In most of tlie earlier studies γ_s was determined by the pyroelectric method. We have adopted the dielectric dispersion method for tlie determination of γ_s. As we have seen in chapter III the generalized mean field model predicts[29] the following relatioris for tlie strength and relaxation frequency of the soft mode (neglecting $\epsilon\mu^2$ term)

$$\epsilon_o \Delta\epsilon_s = \frac{(\epsilon_o C\epsilon)^2}{a(T - T_c) + K_3 q_o^2} \tag{4.21}$$

Table 4.1

P_s/γ_ϕ ratios for the 10th homologue

(at T_c – T = 5°C) of each series

Compound	P_s/γ_ϕ (C/m^2 Pa.S)
A_{10}	0.009
B_{10}	0.008
C_{10}	0.015
D_{10}	0.025
Lactic acid derivatives[2']	0.06
MHPOBC[28]	0.04

$$f_s = \frac{\alpha(T - T_c) + K_3 q_o^2}{2\pi\gamma_s} \tag{4.22}$$

where $\Delta\epsilon_s$ arid f_s are the strength and relaxation frequency of tlie soft mode. C is tlie bilinear coupling term, K_3 an elastic constant, q_o-the helical wave vector at the transition arid a the coefficient of tlie temperature dependent terrn in tlie Landau expansion, ϵ_o the permittivity of the free space and ϵ tlie high temperature dielectric constant.

Multiplying **(4.21)** and **(4.22)**

$$\epsilon_o \Delta\epsilon_s f_s = \frac{\epsilon_o^2 C^2 \epsilon^2}{2\pi\gamma_s} \tag{4.23}$$

or

$$\gamma_s = \frac{\epsilon_o C^2 \epsilon^2}{2\pi\Delta\epsilon_s f_s} \tag{4.24}$$

We have measured the $\Delta\epsilon_s$, f_s and ϵ hy the dielectric method as described in chapter III. Since the coupling coefficient C is not known we define a quantity η as

$$\gamma_s \propto \eta = \frac{\epsilon^2}{2\pi\Delta\epsilon_s f_s} \tag{4.25}$$

The η values computed using eqn. **4.25** are plotted in Fig. **4.20** for the 7th and 12th homologs of the series. Here we have presented the γ_s results in srnectic A phase only. From the figure it is obvious that tlie value of η is more for D_{12} than D_7. But overall temperature variation of η is the same for both tlie compounds indicating that there is no significant change in the rate of variation of η with temperature as the chainlength n is increased.

Figures 4.21 and **4.22** are the arrhenius plots of $\ln\eta$ vs. $\ln(1/T)$ for D_7 and D_{12}. Similar to γ_ϕ, η also behaves in a non-arrhenius fashion close to the transition.

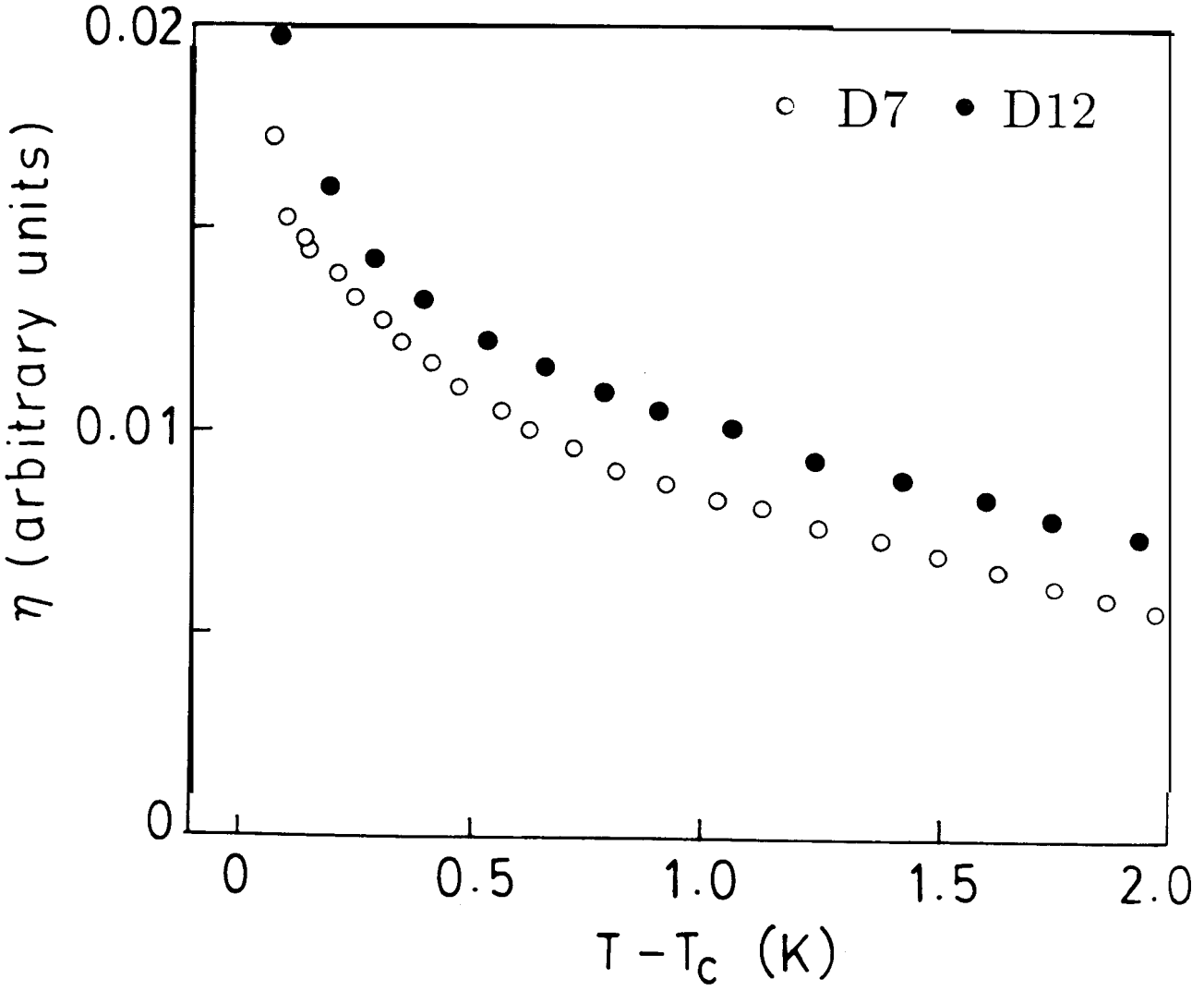

Fig.4.20. Temperature dependence of η for D_7 and D_{12}.

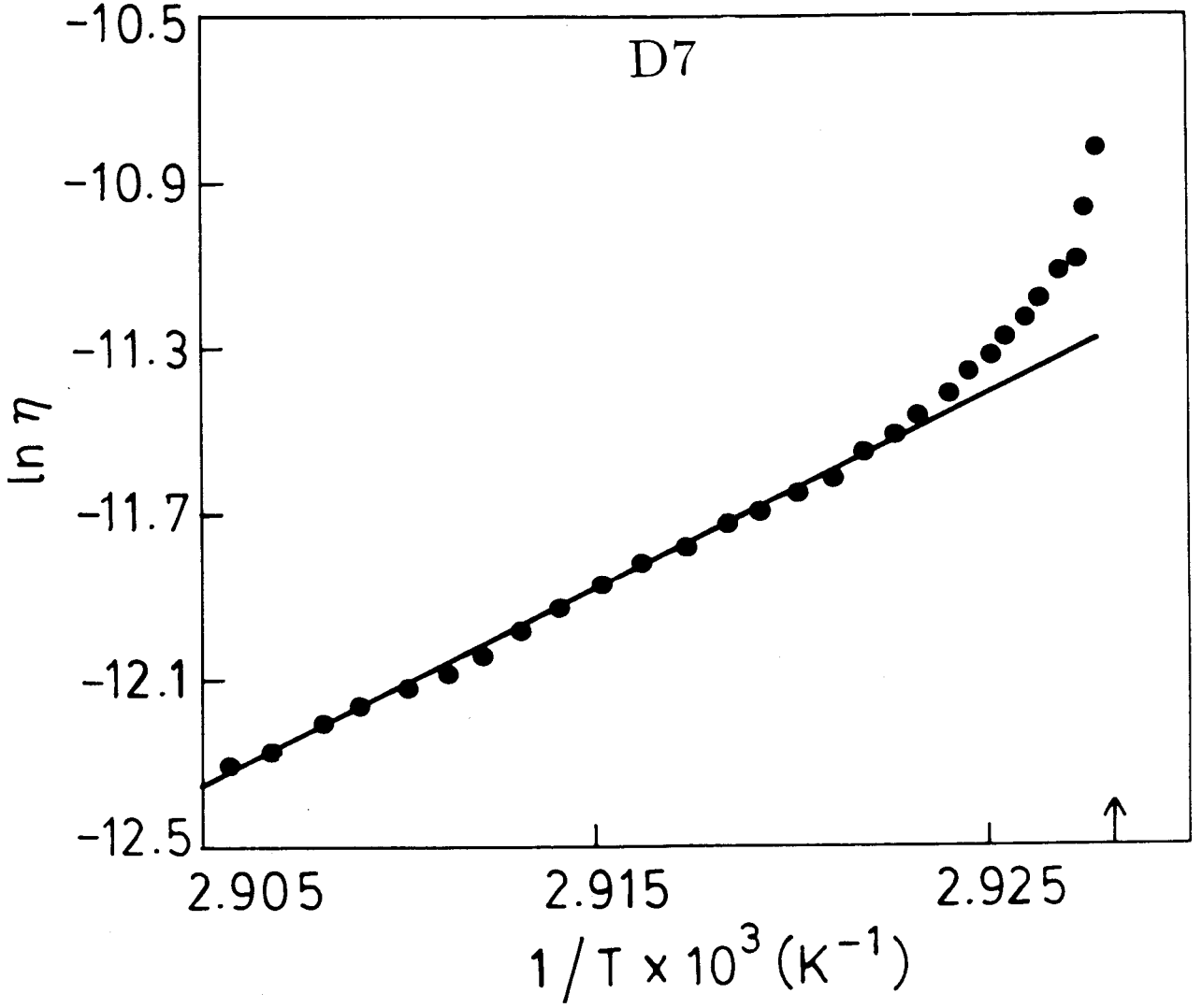

Fig.4.21. Arrhenius plot of η for D_7.

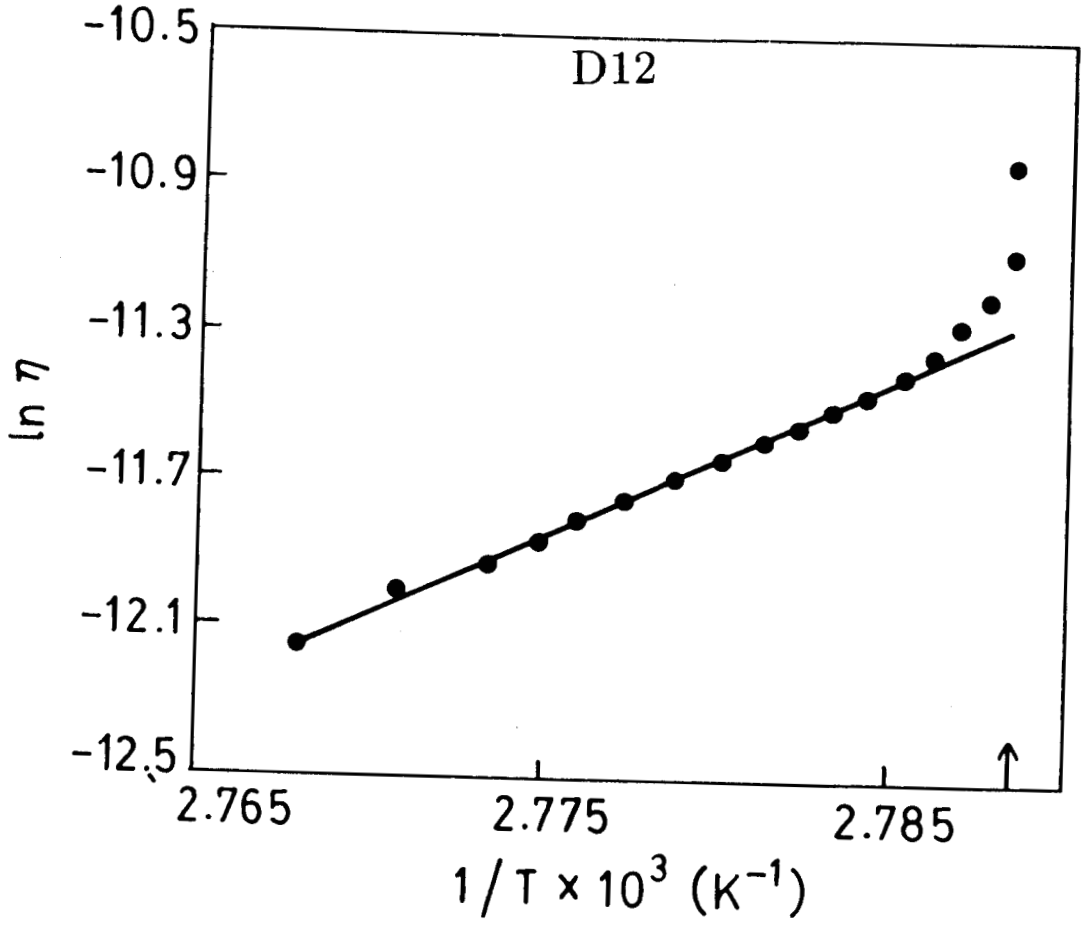

Fig.4.22. Arrhenius plot of η for D_{12}.

For the data away from T_c we have fitted a straight line, the slope of which gives a measure of the activation energy. Within experimental errors, the slopes and thus tlie activation energies for the two compounds are tlie same, indicating that the tilt fluctuations are hardly influenced by the increase in chain length. Since the coupling coefficient is not known, it was not possible to find the absolute value of y,. However we have determined tlie absolute value of γ_s for another compound C_6 (the Gth homologue of the C series; see Table 2.3). For this compound we have obtained y, by the dielectric method. The value of C was obtained by the procedure explained already in chapter III which enabled the determination of y,. We have plotted In γ_s vs. T - T_c in Fig. 4.23. It is seen that γ_s diverges at the transition. We have fitted tlie data of γ_s to an expression of the form

$$\gamma_s = A(T - T_c)^x + \gamma_o \exp(B/T) \tag{4.26}$$

where the last term in RHS is tlie usual arrhenius background contribution. The fit gives a value of x = -0.27. The value of x obtained for this compound is same as that obtained by Gouda et *al.*,[30] for another compound.

We have also determined γ_ϕ and γ_G for this compound by employing tlie hysteresis loop method. A semilog plot of γ_ϕ, γ_G versus $T_c - T$ is shown in Fig. 4.24. Tlie temperature dependence of these two quantities confirms our earlier conclusion that it is γ_G which is of more fundamental importance. Furthermore it is seen, from Fig. 4.23 and 4.21, that the value of γ_s is an order of magnitude greater than the value of γ_ϕ, which is in a good agreement with the results of Pozhidayev *et.al.*[5]

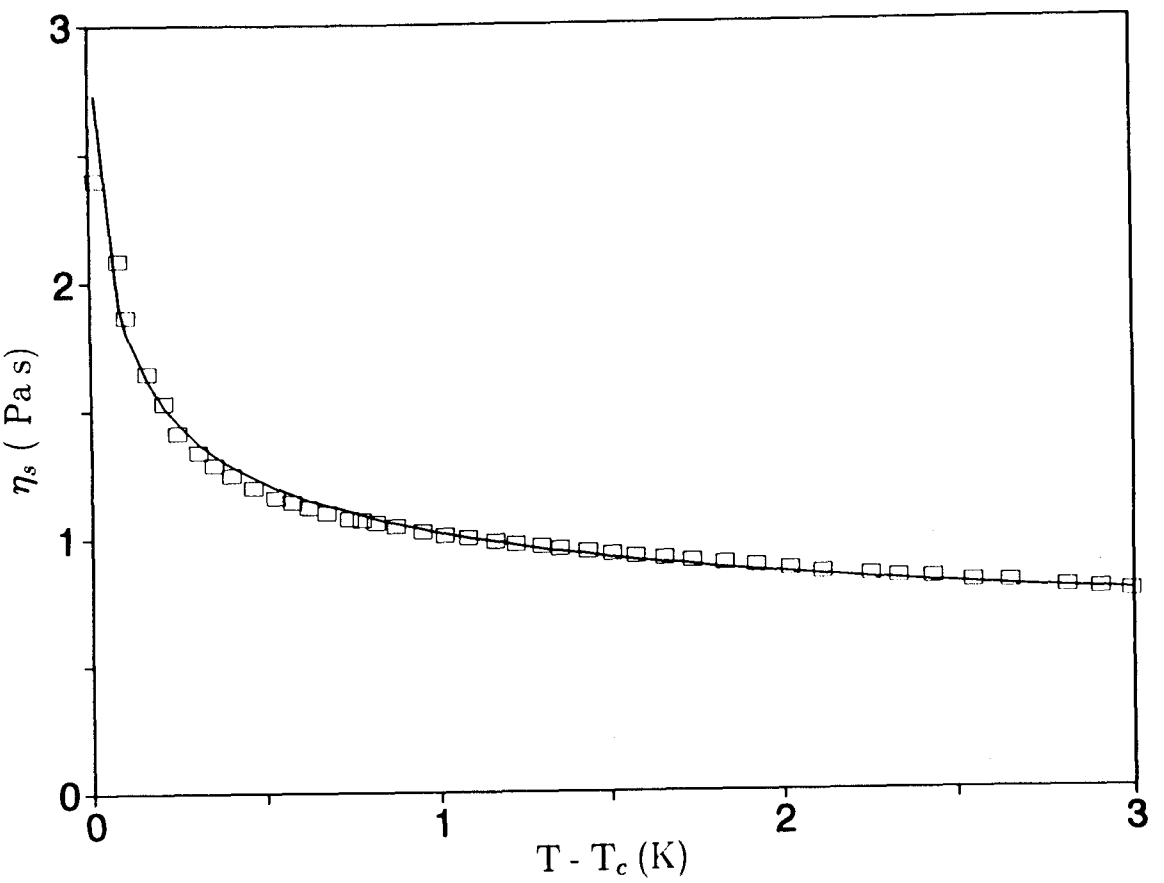

Fig.4.23. Temperature dependence of soft mode viscosity η_s; squares represent the experimental data and the line shows the fit to eqn. (4.26).

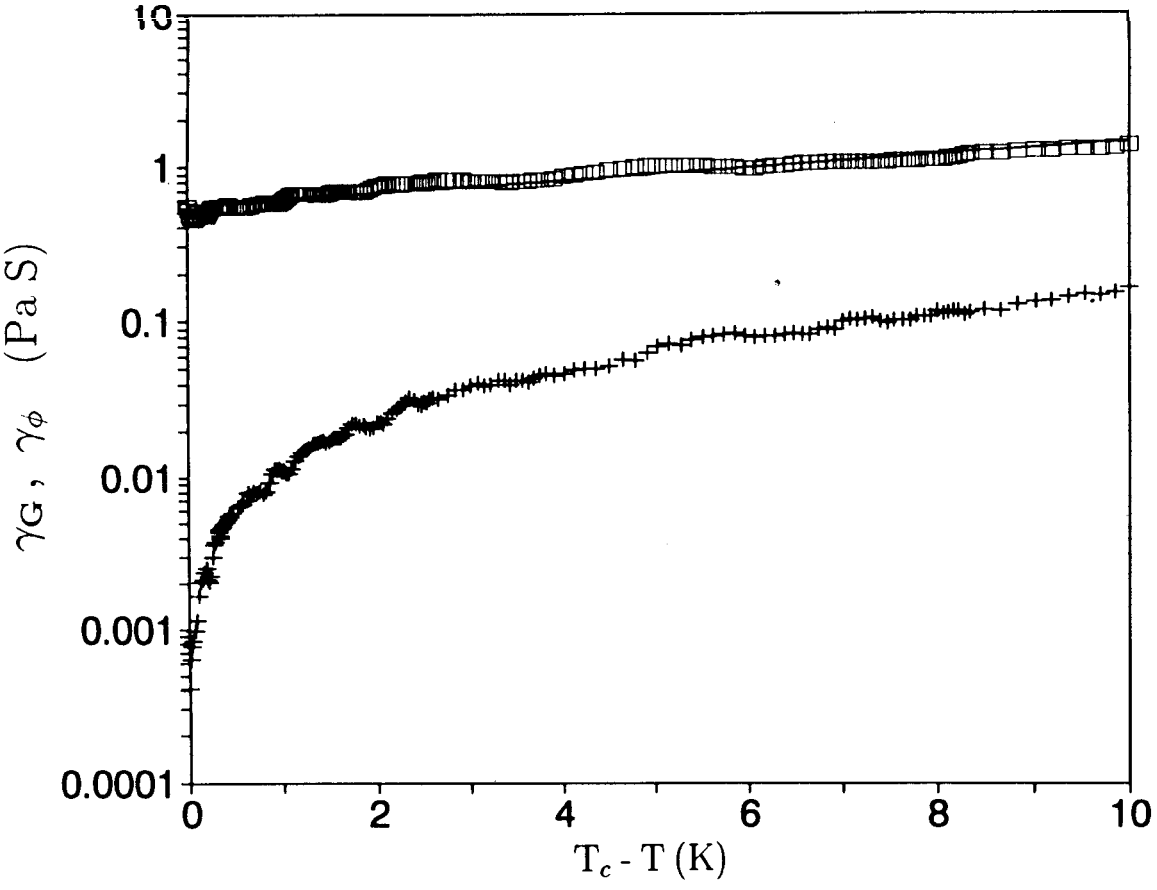

Fig.4.24. Variation of γ_ϕ (+) and γ_G (□) as a function of temperature. Note tliat γ_G shows Arrhenius behaviour right up to the transition.

References

[1] R.B.Meyer, L. Liebert, L.Strzelecki and P.Keller, *J. de Phys. Lett.*, 36, 69 (1975).

[2] N.A.Clark and S.T.Lagerwall, *Appl.* Phys. *Lett.*, 36, 899 (1980).

[3] K.Skarp, *Ferroelectrics*, **84**, 119 (1988).

[4] N.A.Clark, M.A.Handschy and S.T.Lagerwall, *Mol. Cryst. Liquid Cryst.*, 94, 213 (1983).

[5] E.P.Pozhidayev, L.M.Blinov, L.A.Beresnev and V.V.Belyayev, *Mol. Cryst. Liquid Cryst.*, 124, 359 (1985).

[6] K.Skarp, I. Dahl, S.T.Lagerwall and B.Stabler, *Mol. Cryst. Liquid Cryst.*, 114, 283 (1984).

[7] C.Escher, T.Geelhaar and E.Bohm, *Liquid Crystals*, **3**, 469 (1988).

[8] C.Escher, H.R.Dubal, W.Hemmerling, I.Muller, O.Ohlendorf and R.Wingen, *Ferroelectrics*, 84, 89 (1988).

[9] F.Gouda, K.Skarp and S.T.Lagerwall, *Ferroelectrics*, **113**, 165 (1991).

[10] A.Levstik, Z.Kutnjak, C.Filipic, I.Levstik, Z.Bregar, B.Zeks and T.Carlsson, *Phys. Rev.*, A42, 2204 (1990).

[11] K.Skarp, K.Flatischler and S.T.Lagerwall, *Ferroelectrics*, **84**, 183 (1988).

[12] M.Ozaki, T.Hatai, K.Nokao and K.Yoshino, *J. Appl. Phys., 65,* 3602 (1'389).

[13] S.Garoff and R.B.Meyer, Phys. *Rev. Lett.*, 38, 848 (1977).

[14] See for e. g., S.Chandrasekhar, *Liquid Crystals* (Cambridge University Press, 1977).

[15] P.Pieranski, E.Guyon, P.Keller, L.Libert and W.Kuczynski, Mol. *Cryst. Liquid Cryst.*, 38, 275 (1977).

[16] M.I.Barnik, V.A.Bailakov, V.G.Chigrinov arid E.P.Pozhidaev, *Mol. Cryst. Liquid Cryst.*, 143 101 (1987).

[17] K.Flatischler, K.Skarp, S.T.Lagerwall and B.Stabler, *Mol. Cryst. Liquid Cryst.*, 131, 21 (1985).

[18] S.Kimura, S.Nishiyama, Y.Ouchi, H.Takezoe and A.Fukuda, *Japan J. Appl. Phys.*, **26**, L255 (1987).

[19] Xue Jiu Zhi, M.A.Handschy and N.A.Clark, *Ferroelectrics,* **73**, 305 (1987).

[20] I. Dahl, S.T.Lagerwall and K.Skarp, *Phys.* Rev., **A36**, 4380 (1987).

[21] P.Schiller, *Cryst. Res. Technol.*, **21**, 301 (1986).

[22] Xue Jiu-Zhi, hl.A.Handschy and N.A.Clark, *Liquid Crystals*, 2, 707 (1987).

[23] C.B.Sawyer and C.H.Tower, *Phys. Rev.*, **35**, 269 (1930).

[24] H.Diamant, K.Drenck and R.Pepinsky, *Rev. Sci. Instrum.*, 28, 30 (1957).

[25] B.Shivkumar. B.K.Sadashiva, S.Krishna Prasad and S.M.Khened, *Ferroelectrics,* 114, 273 (1991).

[26] C.C.Huang, *Mol. Cryst. Liquid Cryst.*, **144**, 1 (1987).

[27] B.Otterholm, C.Alstermark, K.Flatischler, A.Dahlgren, S.T.Lagerwall and K.Skarp, *Mol. Cryst. Liquid Cryst.*, 146, 189 (1987).

[28] A.D.L.Chandani, Y.Ouchi, H.Takezoe and A.Fukuda, *Japan J. Appl. Phys.*, 27, L276 (1988).

[29] C.Filipic, T.Carlsson, A.Levstik, B.Zeks, R.Blinc, F.Gouda, S.T.Lagerwall and K.Skarp, *Phys. Rev.*, **A38,** 5833 (1988).

[30] F.Gouda, K.Skarp, G.Andersson, H.Kresse and S.T.Lagerwall, *Japan J. Appl. Phys.*, 28, 1887 (1989).